Optics and Lasers in Engineering 51 (2013) 651–655

Contents lists available at SciVerse ScienceDirect

Optics and Lasers in Engineering

journal homepage: www.elsevier.com/locate/optlaseng

Spectral effects of dual wavelength low coherence light source in white light interferometry

Wee Keat Chong [a,*], Xiang Li [a], Yeng Chai Soh [b]

[a] Precision Measurement Group, Singapore Institute of Manufacturing Technology, 71 Nanyang Drive, Singapore 638075, Singapore
[b] School of Electrical and Electronic Engineering, Nanyang Technological University, 50 Nanyang Avenue, Singapore 639798, Singapore

ARTICLE INFO

Article history:
Received 25 September 2012
Received in revised form
27 November 2012
Accepted 24 December 2012
Available online 8 February 2013

Keywords:
Vertical scanning interferometry
Hybrid light source
LED
Fringe contrast function
Spectral manipulation

ABSTRACT

The spectral property of some modern (or hybrid) low coherent light source introduces distinctive feature to the interference signal of white light interferometry. The distinctive feature is defined as discontinuities which make the fringe contrast function (which is the envelope of the interference signal) unable to be modeled as a single Gaussian function. In this paper, we investigate the spectral effect of dual wavelength low coherence light source in white light interferometry and identify the distinctive feature as the result of destructive interference within the localized window where the optical path difference (OPD) is small. By doing so, we give a theoretical explanation of the distinctive feature and demonstrate that the fringe contrast function (and the location of the distinctive feature) can be manipulated by spectrum shaping.

1. Introduction

White light interferometry (which is also known as vertical scanning interferometry or coherence scanning interferometry) is an established optical method for surface height profile measurement. It is done by analyzing a series of interference patterns of low coherence light with known optical path differences (OPDs) among them.

Research in white light interferometry has been focused on the effects of imperfection in the vertical scanning mechanism [1–3] and algorithm for reconstructing height profile from interference signal [4–7]. Other than these, researchers have also studied the effects of dispersion [8], numerical aperture [9], coherence length of light source [10], and vibration [11] on white light interferometry.

Other than being a broadband low coherence light, there is no specific requirement on the light source of white light interferometry. As the conventional white light source has only one peak that is in the Gaussian distribution in its effective spectrum, its corresponding interference signal always has only one high frequency component, and its fringe contrast function (which is the envelope function of the interference signal) can be reasonably modeled as a single Gaussian function [15]. So most prior works [5,12–14] have neglected the spectral effects of the light source.

Driven by advancement in the lighting technology and new application such as dynamic characterization of MEMS, researchers [15–18,19] have been testing various modern and hybrid light sources such as phosphor-based white LED, supercontinuum light and hybrid light source. As shown in Fig. 1, these modern light sources are made out of narrow range of wavelengths in the visible range.

As these modern light sources [15,16,19] are different from the conventional white light source, a distinctive feature (in the interference signal) has been observed [15,16,19,20]. The distinctive feature is defined as discontinuities which make the fringe contrast function unable to be modeled as a single Gaussian function.

For example, Fig. 2 shows the intensity spectrum of a phosphor-based white LED which has two peaks in its intensity spectrum and the corresponding correlogram with the distinctive features highlighted in yellow boxes. With the distinctive features, the envelope of the interference signal cannot be modeled as a single Gaussian function. The effects of the distinctive feature to the reconstructed height profile vary depending on the working principle of the reconstruction algorithm, however it has been shown that the measurement repeatability will degrade if the spectral effect is not treated properly [15].

Researchers [15,16,19,21] have studied and shown that the distinctive feature is related to the low coherent light source with two peaks in its spectrum, but there is no theoretical explanation for it. As such, spectrum shaping for achieving the distinctive feature has been done on the trial-and-error (or ad hoc) approach.

* Corresponding author. Tel.: +65 67932072; fax: +65 67916377.
E-mail address: wkchong@simtech.a-star.edu.sg (W.K. Chong).

0143-8166/$ - see front matter © 2013 Elsevier Ltd. All rights reserved.
http://dx.doi.org/10.1016/j.optlaseng.2012.12.014

In this paper, we investigate the spectral effect of dual wavelength low coherence light source in white light interferometry and identify the distinctive feature (highlighted in Fig. 2(b)) as a result of destructive interference within the localized window where the optical path difference (OPD) is small. By doing so, we give a theoretical explanation of the distinctive feature and demonstrate that the fringe contrast function (and the location of the distinctive feature) can be manipulated by spectrum shaping.

2. Physical model

In a white light interferometry, the light beam from the light source is split into two: one to the reference surface and the other to the measurement surface, then these light beams are reflected and interfere with each other. An interference pattern occurs when the optical path difference (OPD) between these two light beams is small. The interference pattern is known as interferogram, and is recorded by area-based photo-sensitive sensor such as charge-coupled device (CCD) camera. Correlogram is the function of intensity response of each pixel against the OPD, and its envelope function is known as fringe contrast function.

As the interference signal is very sensitive to environmental factors such as vibration and sensor noise, researchers [9,10] used the following physical model to simulate the interference signal for their works.

$$I_{interference}(z) = C_1 \int_{bandwidth} \int_0^{\theta_0} \{k^2 \times \cos[2k(z - z_0)\cos\theta + \phi] \times \sin\theta\cos\theta d\theta\} F(k) dk d\theta \quad (1)$$

where C_1 is the constant, z is the defocus position (which corresponds to the OPD), z_0 is related to the height profile of sample surface, k is the angular wave number ($k = 2\pi/\lambda$), θ_0 is related to the numerical aperture (NA) of the objective lens ($NA = n \sin\theta_0$, where n is the refractive index of the medium in which the lens is working), ϕ is the phase offset, and $F(k)$ is the intensity spectrum of light source.

This physical model is a generalized model which can simulate the effects of intensity spectrum of light source and numerical aperture of objective lens. Although it is capable of simulating the interference signal with distinctive feature (as shown in Fig. 2), it does not help in explaining why and how the distinctive feature is generated. This is because the generalized model is hard to be manipulated algebraically. For example, it is difficult to identify and extract the term(s) representing the OPD range where the interference occurs and the fringe contrast function out of the generalized physical model.

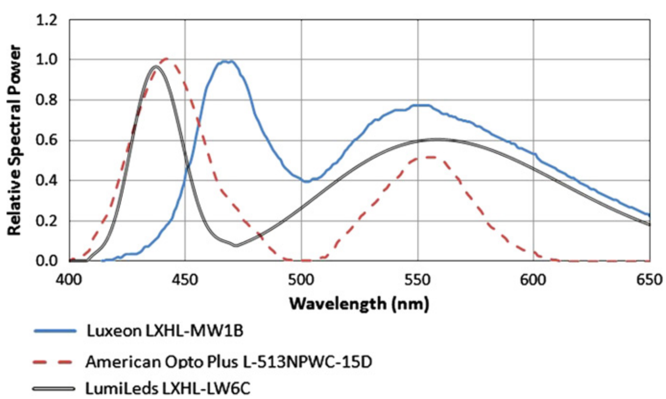

Fig. 1. Spectra of some modern light sources used in the prior works [15,16,19].

3. Proposed theory

3.1. Dual wavelength low coherence light source

First of all, dual wavelength low coherence light source is not necessarily a modern light source. For example, Molnar and Tutsch created a dual wavelength low coherence light by combining a conventional broadband light source and a He–Ne laser with a wavelength of 632.8 nm [21]. Secondly the hybrid light sources in Heikkinen et al.'s work is made out of two monochromatic LEDs [19]. On the other hand, the intensity spectrum of supercontinuum light source (which is an example of modern low coherence light source) is similar to the conventional light source [17,18], and there is no distinctive feature in its corresponding interference signal.

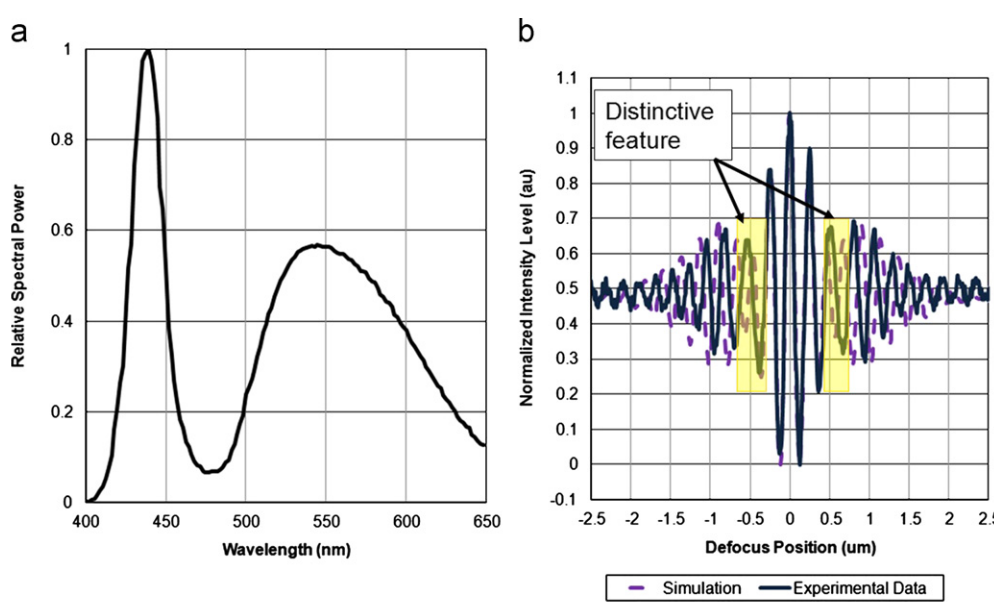

Fig. 2. Graphical illustration of the distinctive feature: (a) spectrum of phosphor-based white LED, LXHL–LW6C and (b) corresponding interference signals (by simulation and experiment) with the distinctive features highlighted in yellow box. (For interpretation of the references to color in this figure legend, the reader is referred to the web version of this article.)

Researchers [15,16,19,21] have shown that the distinctive feature is related to the low coherent light source with two peaks in its spectrum, but there is no mathematical model of the light source. So we first model the light source required to generate the distinctive feature as the dual wavelength low coherence light source which can be represented as follows:

$$f(k) = A_1 e^{-\left(\frac{k-k_1}{\sigma_1}\right)^2} + A_2 e^{-\left(\frac{k-k_2}{\sigma_2}\right)^2} \tag{2}$$

where k is the angular wave number ($=2\pi/\lambda$), A_1 and A_2 are the scaling factors, k_1 and k_2 indicate the peak wave number of each light, and σ_1 and σ_2 indicate the spread of each color in spectral domain. Followed by substituting Eq. (2) into Eq. (1) to derive the corresponding correlogram:

$$\begin{aligned} I(z) = {} & g_1(z-z_0)\cos(2k_1(z-z_0)+\phi_1) \\ & + g_2(z-z_0)\cos(2k_2(z-z_0)+\phi_2) \end{aligned} \tag{3}$$

where z is the defocus position (which corresponds to the OPD), z_0 is related to the height profile of sample surface, k is the equivalent wave number of light ($k=2\pi/\lambda$), ϕ is the phase offset and g is the fringe contrast function. The shape of the fringe contrast function is a Gaussian function, and the spread of the Gaussian function is subjected to the numerical aperture of objective lens and the intensity spectrum of light source. As there are two dominant colors in the spectrum of the light source, so there are g_1, g_2, k_1, k_2 etc.

With the correlogram of the dual wavelength low coherence light source derived, it is found that the correlogram is similar to a beat. A beat is interference between two waves of very similar frequencies, and mathematically it can be represented as follows:

$$\begin{aligned} & \cos(2\pi f_1 t) + \cos(2\pi f_2 t) \\ & = 2\cos\left(\frac{2\pi(f_1-f_2)t}{2}\right)\cos\left(\frac{2\pi(f_1+f_2)t}{2}\right) \\ & = 2\cos\left(2\pi\frac{\Delta f}{2}t\right)\cos\left(2\pi f_{average}t\right) \end{aligned} \tag{4}$$

where f is the frequency, t is the independent variable, $f_{average}$ is equal to $(f_1+f_2)/2$, Δf *is* equal to (f_1-f_2), and $\Delta f/2$ is the beat frequency.

Next, we re-arrange and express the corresponding correlogram (Eq. (3)) in the form of beat. For simplicity and tidiness of derivation, it is assumed that $g_1=g_2=g$, $\phi_1=\phi_2=0$ and $z_0=0$, the corresponding correlogram is re-arranged as follows:

$$\begin{aligned} I(z) & = g(z)\left[\cos(2k_1 z)+\cos(2k_2 z)\right] \\ & = g(z)\left[2\cos\left(\frac{2(k_1-k_2)z}{2}\right)\cos\left(\frac{2(k_1+k_2)z}{2}\right)\right] \\ & = g(z)\left[2\cos(\Delta k z)\cos(2k_{average}z)\right] \end{aligned} \tag{5}$$

where k is the wave number ($k=2\pi/\lambda$), $k_{average}$ is equal to $(k_1+k_2)/2$ and Δk is equal to (k_1-k_2).

As the distinctive feature (shown in Fig. 2(b)) cannot be explained by the sub fringe contrast functions (g_1 and g_2 in Eq. (3)) and Eq. (5) suggests interference, we propose that the distinctive feature is due to interference between the high frequency components (k_1 and k_2 in Eq. (2)). A destructive interference between these two high frequency components would result in a dip in the effective correlogram, matching the definition of the distinctive feature.

3.2. Verification

To verify the proposed theoretical explanation, we apply it on phosphor-based white LED which distinctive feature was first investigated [15]. The intensity spectrum of the phosphor-based white LED is shown in Fig. 2(a), k_1 and k_2 are 14.3 rad/μm (440 nm) and 11.4 rad/μm (550 nm) respectively, σ_1 and σ_2 are 0.4941 rad/μm and 1.439 rad/μm respectively and A_1/A_2 is around 1.6. The wrapped phase distribution of these two high frequency components is recovered by the Fourier Transform Method [22] and expressed as follows:

$$\begin{aligned} \Phi_1 & = (2k_1(z-z_0)+\phi_1)\%2\pi \\ \Phi_2 & = (2k_2(z-z_0)+\phi_2)\%2\pi \end{aligned} \tag{6}$$

where % is the modulus operator.

As shown in Fig. 3, the location of the distinctive feature is in the region (where the defocus position is between 0.35 μm and 0.8 μm) where there are destructive interferences. This shows that the proposed explanation is valid and the distinctive feature is due to the occurrence of destructive interferences within the localized window where the OPD is small.

4. Manipulating fringe contrast function by spectrum shaping

With the proposed explanation, knowledgeable spectrum shaping to manipulate the fringe contrast function (and the distinctive feature) is now feasible. With reference to Eq. (6), the location of total destructive interference between two colors can be determined by solving

$$\Phi_1 = \Phi_2 + \pi \tag{7}$$

By assuming $k_1 > k_2$, $z_0=0$, and $\phi_1=\phi_2$, the location of the total destructive interference (which corresponds to the distinctive feature) can be expressed as follows:

$$\begin{aligned} & 2k_1 z = 2k_2 z + \pi \\ & \quad 2k_1 z - 2k_2 z = \pi \\ & \quad (k_1-k_2)z = \frac{\pi}{2} \\ & \quad z = \frac{\pi}{2(k_1-k_2)} \end{aligned} \tag{8}$$

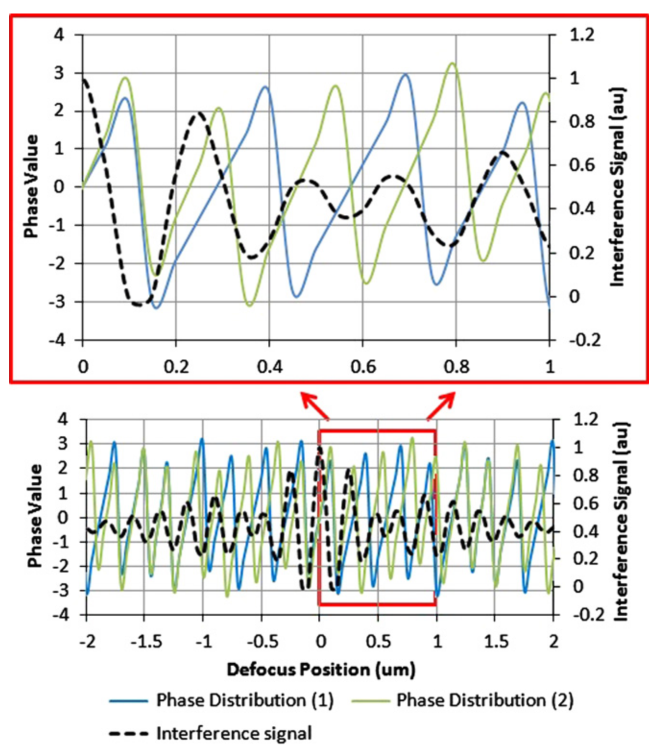

Fig. 3. Graphical illustration that the distinctive feature is the result of destructive interference between two colors (which are blue and yellow light for phosphor-based white LED). (For interpretation of the references to color in this figure legend, the reader is referred to the web version of this article.)

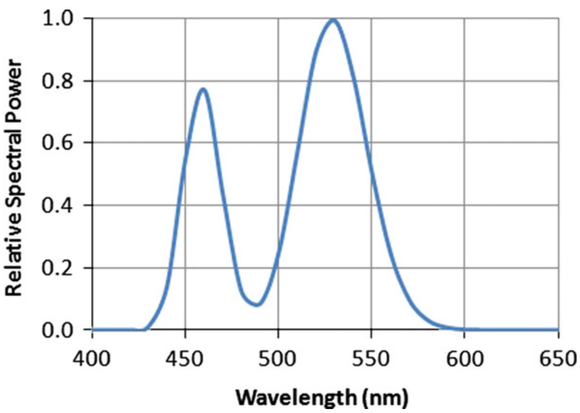

Fig. 4. Effective spectrum of the hybrid light source used to shift the location of the distinctive feature away from the zero OPD location.

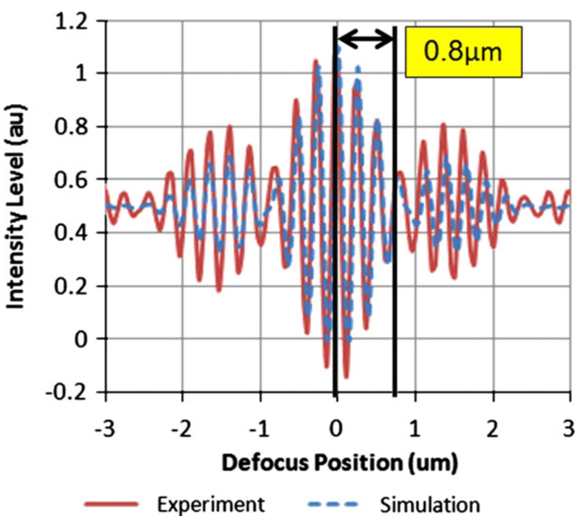

Fig. 5. Evaluating the accuracy of the proposed explanation in controlling/predicting the location of the distinctive feature: by simulation and experimental verification, the location of the feature is around 0.8 μm (with respect to the zero OPD location) while the location estimated by the proposed explanation is 0.88 μm.

Based on Eq. (8), the location of the distinctive feature with respect to the zero OPD location is inversely proportional to the difference between the wave number of two colors (which is (k_1-k_2) in Eq. (8)). If the difference is too small, the distinctive feature will occur outside the localized region (where interference occurs) and will not be observable. Meanwhile, the difference between the wave number of two colors is limited to the finite spectral sensitivity of detector.

4.1. Experimental verification

As a demonstration and verification, we create a hybrid light source (which consists of two monochromatic LEDs) to shift the location of the distinctive feature away from the zero OPD location. The hybrid light source is made out of blue (LXHL–LB5C) and green (LXHL–LM5C) LEDs to create an effective spectrum as shown in Fig. 4. The dominant wavelengths are 528 nm (11.9 rad/μm) and 458 nm (13.71 rad/μm) , and the blue–green ratio is 0.78:1.

With the effective spectrum of hybrid source shown in Fig. 4, the proposed explanation estimates the location of the distinctive feature is around 0.88 μm away from the zero OPD location. With simulation and physical experiment, the location of the distinctive feature is found to be around 0.8 μm away from the zero OPD location. The estimation by the proposed explanation (which is 0.88 μm) agrees with the simulation and experiment results (which are around 0.8 μm), see Fig. 5.

It is shown that the proposed explanation is accurate and can be applied to manipulate/predict the location of the distinctive feature.

5. Conclusion

In summary, we investigated the spectral effect of dual wavelength low coherence light source in white light interferometry and identified the distinctive feature (which makes the fringe contrast function of white light interferometry unable to be modeled as a single Gaussian function) as the result of destructive interference within the localized window where the optical path difference (OPD) is small. By doing so, we gave a theoretical explanation of the distinctive feature and demonstrated that the fringe contrast function (and the location of the distinctive feature) can be manipulated with a hybrid light source which is made out of blue and green LEDs.

Future research includes improving the proposed explanation to consider the amplitude of the distinctive feature and designing a height reconstruction algorithm which harnesses the distinctive feature.

References

[1] Kiyono S, Gao W, Zhang S, Aramaki T. Self-calibration of a scanning white light interference microscope. Opt Eng 2000;39:2720–5.
[2] Crescentini L. Fringe pattern analysis in low-quality interferograms. Appl Opt 1989;28:1231–4.
[3] Schmit J, Olszak A. High-precision shape measurement by white-light interferometry with real-time scanner error correction. Appl Opt 2002;41:5943–50.
[4] Gurov I, Ermolaeva E, Zakharov A. Analysis of low-coherence interference fringes by the Kalman filtering method. J Opt Soc Am A 2004;21:242–51.
[5] Ai C, Novak EK. Centroid approach for estimating modulation peak in broad-bandwidth interferometry. US patent 5633715 (n.d.).
[6] Larkin KG. Efficient nonlinear algorithm for envelope detection in white light interferometry. J Opt Soc Am A 1996;13:832–43.
[7] Hirabayashi A, Ogawa H, Kitagawa K. Fast surface profiler by white-light interferometry using a new algorithm, the SEST algorithm. Opt Manuf Test IV SPIE 2001;4451:356–67.
[8] Pavliček P, Soubusta J. Measurement of the influence of dispersion on white-light interferometry. Appl Opt 2004;43:766–70.
[9] Sheppard CJR, Larkin KG. Effect of numerical aperture on interference fringe spacing. Appl Opt 1995;34:4731–4.
[10] de Groot P, Colonna de Lega X. Signal modeling for low-coherence height-scanning interference microscopy. Appl Opt 2004;43:4821–30.
[11] Chen LC, Tapilouw AM, Yeh SL, Lin ST, Chen JL, Huang HC. Development of innovative fringe locking strategies for vibration-resistant white light vertical scanning interferometry (VSI). Key Eng Mater 2010;437:89–94.
[12] Chim SSC, Kino GS. Correlation microscope. Opt Lett 1990;15:579–81.
[13] de Groot P, Deck L. Surface profiling by analysis of white-light interferograms in the spatial frequency domain. J Mod Opt 1995;42:389–401.
[14] LiM, Quan C, Tay CJ, Reading I, Wang S. Measurement of transparent coating thickness by the use of white light interferometry, In: Proceedings of the third international conference on experimental mechanics and third conference of the asian committee on experimental mechanics; 2005. vol. 5852, p. 401–6.
[15] Heikkinen V, Aaltonen J, Kassamakov I, Wälchli B, Räikkönen H, Paulin T, et al. Non-phosphor white LED light source for interferometry,. Proc of SPIE 2011;8133:813309, http://dx.doi.org/10.1117/12.893691.
[16] Hanhijärvi K, Kassamakov I, Heikkinen V, Aaltonen J, Sainiemi L, Grigoras K, et al. Stroboscopic supercontinuum white-light interferometer for MEMS characterization. Opt Lett 2012;37:1703–5.
[17] Kassamakov I, Hanhijärvi K, Abbadi I, Aaltonen J, Ludvigsen H, Hæggström E. Scanning white-light interferometry with a supercontinuum source. Opt Lett 2009;34:1582–4.
[18] Chong WK, Li X, Wijesoma S. Effects of phosphor-based LEDs on vertical scanning interferometry. Opt Lett 2010;35:2946–8.

[19] Heikkinen V, Hanhijärvi K, Aaltonen J, Räikkönen H, Wälchli B, Paulin T, et al. Hybrid light source for scanning white light interferometry-based MEMS quality control. Proceedings of SPIE 2011;8082:80822O.

[20] Hanhijärvi K, Aaltonen J, Kassamakov I, Grigoras K, Sainiemi L, Franssila S, et al. Effect of LED spectral shift on vertical resolution in stroboscopic white light interferometry. Proc of SPIE 2008;7003 70031S, http://dx.doi.org/10.1117/12.780972.

[21] Molnar G, Tutsch R. Vertical scanning interferometry with a mixed-coherence light source. In: Osten W, Gorecki C, Novak EL, editors. Optical measurement systems for industrial inspection V, vol. 6616. SPIE; 2007. p. 661608-7.

[22] Takeda M, Ina H, Kobayashi S. Fourier-transform method of fringe-pattern analysis for computer-based topography and interferometry. J Opt Soc Am 1982;72:156–60.